Articles in PresS. J Appl Physiol (October 1, 2004). doi:10.1152/japplphysiol.00590.2004

JAP-00590-2004

Mechanics, nonlinearity, and failure strength of lung tissue in a mouse model of emphysema: possible role of collagen remodeling

Satoru Ito, Edward P. Ingenito*, Kelly K. Brewer, Lauren D. Black,

Harikrishnan Parameswaran, Kenneth R. Lutchen, and Béla Suki

Department of Biomedical Engineering, Boston University, Boston MA 02215,

*Division of Pulmonary and Critical Care Medicine, Brigham and Women's Hospital,

Harvard Medical School, Boston MA 02115

Running title: Respiratory mechanics of emphysema

Address for correspondence and proofs:

Béla Suki, Ph.D.

E-mail: bsuki@bu.edu

Department of Biomedical Engineering, Boston University

44 Cummington Street, Boston MA 02215

TEL: 1-617-353-5907

FAX: 1-617-353-6766

ABSTRACT

Enlargement of the respiratory airspaces is associated with the breakdown and re-organization of the connective tissue fiber network during the development of pulmonary emphysema. In this study, a mouse (C57BL/6) model of emphysema was developed by direct instillation of 1.2 IU of porcine pancreatic elastase (PPE) and compared with control mice treated with saline. The PPE-treatment caused 95% alveolar enlargement ($P = 0.001$) associated with a 29% lower elastance along the quasi-static pressure-volume curves ($P < 0.001$). Respiratory mechanics were measured at several positive end-expiratory pressures in the closed chest condition. The dynamic tissue elastance was 19% lower ($P < 0.001$), hysteresivity was 9% higher ($P < 0.05$), and harmonic distortion, a measure of collagen-related dynamic nonlinearity, was 33% higher in the PPE-treated group ($P < 0.001$). Whole lung hydroxyproline content, which represents the total collagen content, was 48% higher ($P < 0.01$), and α-elastin content was 13% lower ($P = 0.16$) in the PPE-treated group. There was no significant difference in airway resistance ($P = 0.7$). The failure stress at which isolated parenchymal tissues break during stretching was 40% lower in the PPE-treated mice ($P = 0.002$). These findings suggest that following elastolytic injury, abnormal collagen remodeling may play a significant role in all aspects of lung functional changes leading to progressive emphysema.

214 words

Keywords: elastance; extracellular matrix; failure stress; resistance

INTRODUCTION

Pulmonary emphysema is characterized by permanent destruction of the respiratory bronchioles, alveolar ducts, and alveolar walls, which leads to hyperexpansion and loss of elastic recoil (1). The most widely accepted hypothesis of how tissue destruction occurs in emphysema is that an imbalance of protease and anti-protease activity exists within the lung that ultimately leads to enzymatic degradation of elastin (38, 45). However, changes consistent with emphysema can also result from abnormality of the collagen matrix (4, 8, 12, 21, 23, 25, 35, 49). Recent studies have provided evidence that significant remodeling of the extracellular matrix (ECM) including collagen, elastin, and proteoglycans occurs during the development of emphysema both in humans (4, 12, 48, 49) and in experimental rodent models (12, 21, 25, 52). Therefore, besides elastin degradation, the biological breakdown and subsequent remodeling of collagen during the abnormal repair of the lung tissue would play a role both in the progress of this disease (24, 52) and the physiological functioning of the lung (21, 44).

Among the constituents of the ECM components, elastin and collagen appear to account for most of the viscoelastic mechanical properties of the lung tissue strips (33, 46, 53). Elastic fibers behave more linearly than collagen fibers (28, 36). Therefore, one would predict that the nonlinear behavior of the lung could change when alterations occur in the relative amounts of elastin and collagen in the connective tissue.

We hypothesized that if alterations occur in the collagen fiber network during the development and progress of emphysema, then both the nonlinear viscoelastic properties of the lung tissue and the strength of alveolar walls should change. To test this hypothesis, we measured the nonlinear and viscoelastic properties of the whole lung in a mouse model of emphysema induced by direct instillation of porcine pancreatic elastase (PPE) (26). To characterize lung elasticity and airway function, we measured the quasi-static

pressure-volume (P-V) curves and the forced oscillatory impedance of the respiratory system. We calculated a dynamic nonlinearity index, called harmonic distortion (42), as well as measured the failure stress of parenchymal tissue strips. Finally, to assess changes in composition, we also determined the total amounts of elastin and collagen in the lung.

METHODS

Animal Preparation

Two groups of male C57BL/6 mice (Charles River, Boston, MA), weighing 23 - 25 g were studied. Animals were treated with direct instillation of either 1.2 IU porcine pancreatic elastase (PPE) (Sigma, St. Louis, MO) dissolved in 90 μl of sterile saline (n = 18) or the same amount of saline (control) (n = 18) (26). Three weeks after the treatment, the following experiments were performed. All animal procedures were approved by the Animal Care and Use Committees of Boston University and Harvard Medical School.

Measurement of Respiratory Mechanics

The detailed methods are described elsewhere (20). The control (n = 8) and PPE-treated (n = 9) mice were deeply anesthetized by intraperitoneal injection of pentobarbital (70 mg/kg), tracheostomized, and cannulated in the supine position. The cannula was connected to a computer-controlled ventilator (Flexivent, SCIREQ, Montreal, Canada). Mice were mechanically ventilated with room air using a tidal volume of 8 ml/kg at a frequency of 240 breaths/min. After stabilization, the quasi-static pressure-volume (P-V) curve of the respiratory system was measured as follows. After inflation of the lungs to total lung capacity, defined as a tracheal pressure of 25 cmH_2O, mice were mechanically ventilated under the same condition for 5 sec. Following 3 sec of delay, slow volume inflation (0.1 ml/sec, total 1.2 ml) starting from end-expiratory lung volume was

performed using the computer-controlled ventilator without applying positive end-expiratory pressure (PEEP) (21). Dynamic respiratory mechanics were measured at four different PEEP levels (0, 3, 6, and 9 cmH_2O) in the closed chest condition and assessed by measuring impedance data during forced oscillations. To standardize volume history, each measurement was preceded by two consecutive inflations of the lungs to total lung capacity.

Impedance Measurements

Impedance data collection was made by interrupting mechanical ventilation for 6 s using the optimal ventilation waveform (OVW), which is a broad-band waveform containing energy from 0.5 to 15 Hz as described previously (27). The frequencies in the OVW are selected according to a non-sum non-difference criterion, which eliminates harmonic distortion and minimizes cross talk among the frequencies that are present in the input flow waveform and hence provides smooth estimates of the input impedance (43). The volumes delivered are similar to normal spontaneous tidal volume values and hence the method provides information on the mechanical properties during conditions mimicking breathing. In our experiment, we matched the peak-to-peak OVW amplitude to the tidal volume delivered by the mechanical ventilator. The ventilator displacement and cylinder pressure signals were low-pass filtered at 30 Hz and sampled at 256 Hz. With the use of Fourier analysis, impedance spectra were calculated on overlapping blocks of pressure and flow data as the ratio of the cross-power spectrum of pressure and flow and the autopower spectrum of flow. The forced-oscillatory system was calibrated by measuring the input impedance of known analogs including tubes and bottles with known impedances. The frequency response of the system was obtained, and the measured impedance spectra were off-line corrected for any phase difference between pressure and

flow. Additionally, the flow-dependent impedance of the tracheal cannula was characterized separately and removed from the respiratory impedance of the mice (20).

Mathematical Modeling

Data were analyzed with a model that allows for specific alterations in the lung tissue similar to what might be expected in emphysema. Specifically, we applied a heterogeneous tissue elastance model of the lung (20). Briefly, in this model, we represented the airway tree by a set of airway pathways arranged in parallel, where each compartment is composed of an airway resistance (R_{aw}), an inertance (I_{aw}), and a linear tissue impedance (Z_{Lti}) connected in series. Hantos et al. (16) introduced the constant-phase model and described the Z_{Lti} as:

$$Z_{Lti}(\omega_n) = (G - jH)/\omega_n^{\alpha}, \text{ with } \alpha = 2/\pi \arctan(H/G) \text{ and } \omega_n = \omega/\omega_0 \quad \text{(Eq. 1)}$$

where ω_n and ω are the normalized and absolute circular frequency, G and H are the coefficients of tissue damping and elastance, respectively, *j* is the imaginary unit, and the exponent α describes the frequency dependence of tissue resistance ($R_{ti} = G/(\omega/\omega_0)^{\alpha}$) and tissue elastance ($E_{ti} = H(\omega/\omega_0)^{1-\alpha}$). The normalization factor $\omega_0 = 1$ rad/sec is introduced in order to obtain meaningful units for the parameters G and H (3). The impedance of the airways (Z_{aw}) in each pathway is given by:

$$Z_{aw}(\omega_n) = R_{aw} + j\omega_n I_{aw} \quad \text{(Eq. 2)}$$

The R_{aw}, I_{aw} and hysteresivity (14), defined as the ratio of $\eta = G/H$, of the tissue elements were the same in each pathway while the elastance (H) of the tissue elements followed a hyperbolic distribution between a minimum (H_{min}) and a maximum (H_{max}). The input impedance Z of the network is obtained as (20):

$$Z_{in} = \frac{FZ_{aw}}{F + \ln\left(\frac{Z_{Lti,\min} + Z_{aw}}{Z_{Lti,\max} + Z_{aw}}\right)} \quad \text{(Eq. 3)}$$

where F, $Z_{Lti,min}$ and $Z_{Lti,max}$ are given by $F = \ln(H_{max}/H_{min})$, $Z_{Lti,min}(\omega_n) = (\eta - j)H_{min}/\omega_n^{\alpha}$, and $Z_{Lti,max}(\omega_n) = (\eta - j)H_{max}/\omega_n^{\alpha}$.

By minimizing the root mean square difference between the model and the data (6) the five parameters (R_{aw}, I_{aw}, η, H_{min}, and H_{max}) were determined. The mean H value (H_{mean}) was estimated as the expected value of the distribution function and was calculated from the estimates of H_{min} and H_{max} as:

$$H_{mean} = \frac{H_{max} - H_{min}}{F} \quad \text{(Eq. 4)}$$

The tissue damping, G, was calculated as $G = \eta H_{mean}$.

Dynamic Nonlinearity of Respiratory Mechanics

When applying a broad-band input, one way to probe system nonlinearity is to measure how the elastic and viscous moduli depend on the amplitude of the input. Another way of quantifying nonlinearity is via the so-called harmonic distortion index, which estimates the amount of both harmonic distortion and cross talk in the output signal resulting from system nonlinearities (42). For a broadband input, the coefficient of harmonic distortion K_d is defined as (54):

$$K_d = \sqrt{P_{NI}/P_{TOT}} \times 100\ (\%) \quad \text{(Eq. 5)}$$

where P_{TOT} is the total power in the output and P_{NI} is the output power due to system nonlinearities only, i.e., the power at non-input frequencies. Since only nonlinearities and noise can produce output energy at non-input frequencies, the values of K_d were also corrected for nonzero energy at non-input frequencies (54). The advantage of using K_d is that it can be calculated from a single impedance measurement, whereas the traditional method of characterizing nonlinearity requires the measurement of the moduli at several

distinct amplitudes. The K_d in a linear system is zero. In a nonlinear system driven by sinusoidals, the K_d measures the distortion and crosstalk due to system nonlinearities.

Measurements of Mechanical Failure of Lung Tissues

To assess the strength of the alveolar wall in the parenchyma, failure test of lung tissue strips were carried out. Following the measurements of respiratory function, an additional dose of pentobarbital (70 mg/kg) was injected intraperitoneally to each animal (n = 6 in each group), the thorax was opened, and the animals were exanguinated by severing the inferior vena cava. The heart, lungs, and trachea were carefully resected en bloc and rinsed in phosphate-buffered saline (PBS) (Sigma). The experimental set up was described previously (53). Parenchymal tissue strips having dimensions of 2.0 - 3.0 mm x 0.7 - 1.0 mm x 0.7 - 1.0 mm in length, width and thickness, respectively, were carefully prepared from each lung and the pleura were removed with the use of a razor. Each end of the tissue strip was fixed by cyanoacrylate glue to small metal plates attached to straight steel wires. The assembly was placed in a horizontal tissue bath filled with PBS at room temperature, with one wire attached to a computer-controlled lever arm containing a force transducer (Model 300B, Aurora, ON, Canada). We followed the method reported by Tanaka and Ludwig (47). Briefly, each strip was stretched at a rate of 0.2 mm/sec until the sample separated into two pieces. Due to the limitation of the maximum displacement of the level arm, the strips were first stretched to approximately 3 times their unstretched length before the recording of the displacement and force signals was started. The strain was defined as the total displacement in length normalized by the unstretched length of the samples. A transient decrease in the force (see arrows in Fig. 8) was defined as “the failure stress”, indicating that fibers in the alveolar walls started to break during

stretching. Two or three strips were prepared and measured from each animal, and the average value of the failure stress was used for statistical analysis.

Bronchoalveolar Lavage

Whole lung lavages were performed with 1 ml of PBS twice via the tracheal cannula following the impedance and P-V curve measurements (n = 5 in each group). The return volume was measured, and the bronchoalveolar lavaged fluid (BALF) was centrifuged. The cell pellet was re-suspended in red blood cell lysis buffer (0.01% NH_4Cl) and brought up to the initial lavaged return volume for total cell count by hemocytometry. Slides containing 500 - 1000 cells were prepared using a cytocentrifuge, and stained with rapid Wright's stain. Differential cell analysis was performed by manual counting under a light microscope.

Lung Histology and Morphometry

After mediastinal dissection, the lungs were perfused with 10% buffered formalin via the tracheal cannula at an airway pressure of 25 cmH_2O for at least 20 min (n = 5 in each group). The fixed lungs were embedded in paraffin, sectioned and stained with hematoxylin and eosin for histological analysis. We calculated the average distance between alveolar walls, the mean linear intercept (MLI), according to established methods (10) using a light microscope. For each pair of lungs, 10 histological fields were evaluated.

BALF Elastase-like Activity

Elastase-like activity in BALF was measured using the protocol by Dhami et al. (9). Briefly, BALF samples were lyophilized and reconstituted in water to make a fivefold

concentrated solution. An assay buffer of 0.2 M Tris · HCl, pH 8.0, was prepared and then, 100 µl of assay buffer, 50 µl of substrate (0.5 mg/ml of *N*-succinyl-Ala-Ala-Ala-*p*-nitroanilide), and 50 µl of BALF were added. All samples were assayed in duplicate. EDTA (10 mM) was added to the samples to inhibit metalloelastase (13). Negative control of 150 µl of assay buffer and 50 µl of substrate were used. We assessed background absorbance of each BALF sample by incubating 150 µl of assay buffer with 50 µl of each sample. This value was then subtracted from the absorbance of the test wells. The absorbance of the wells is measured at 405-nm wavelength using a spectro-photometer.

Whole Lung Collagen Content

Collagen content was assessed by measuring the hydroxyproline content of the tissue as previously described by Woessner (51). Lungs from the control (n = 7) and the PPE-treated (n = 7) mice were lyophilized for 12 h to dry weight, measured, minced. The lung sample was then hydrolyzed with 4 ml of 6 N HCl at 100°C for 6 h. One ml of the hydrolysate was then taken and evaporated. The powder was reconstituted with 1 ml of distilled H_2O (dH_2O) and re-evaporated. The powder was then reconstituted with 5 ml of dH_2O. Hydroxyproline (Sigma) standard solutions of 0 - 10 µg/ml were prepared. Sample solution (2 ml) was taken and oxidized with 1 ml of Chloramine-T (Sigma) for 20 min. The reaction was then stopped with 1 ml of 3.15 M perchloric acid. After 5 min, 1 ml of *p*-dimethylaminobenzaldehyde solution was added. The sample was vortexed, incubated in a 60°C bath, and then cooled under tap water for 5 min. The absorbency of the solutions was determined at 557 nm using a spectro-photometer. The hydroxyproline concentration was determined from the standard curve.

Whole Lung Elastin Levels

The lyophilized was placed into 1 ml of 0.25 M oxalic acid. The suspension was then heated at 100°C for 1 h. The specimen was centrifuged, and the supernatant was collected. The above procedure was repeated for a total of five times until all the insoluble elastin had been converted into a soluble product (α-elastin) (7). One ml of the collected supernatants for each mouse was then dialyzed against water using 15,000 molecular-weight cutoff dialysis membrane (Spectrum, Huston, TX). The levels of α-elastin were then determined using Fastin-elastin assay (Biocolor, Belfast, N. Ireland) following the specific protocol outlined in the kit.

Statistical Analysis

All data were expressed as means ± standard deviation (SD). Student's *t*-test and repeated-measure two-way analysis of variance were used to evaluate the significance of differences between means and variances, with $P < 0.05$ as the level of significance.

RESULTS

Histopathology

Fig. 1A and B shows representative alveolar structures of a control and a PPE-treated lung stained with hematoxylin and eosin three weeks following initial treatment. Significant enlargement of the alveolar air spaces was observed in lung samples from PPE-treated mice compared to control. Both the mean and the SD of the MLI in the PPE-treated group (83 ± 21 μm) were significantly larger than in the control group (43 ± 3 μm)($P = 0.001$). There were no significant differences in body weight between PPE-treated (24.9 ± 0.9 g) and control groups (25.2 ± 1.1 g).

BALF Analysis

There were no significant differences in BALF total cell numbers between PPE-treated ($3.4 \pm 1.0 \times 10^4$ /ml) and control groups ($3.8 \pm 0.9 \times 10^4$ /ml) and over 95% of the cells were macrophages in both groups. No eosinophils and only 0.5% neutrophils were observed in both groups. Additionally, no elastase-like activity was detected in BALF of the control and PPE-treated mice, suggesting that direct elastolytic activity of PPE had already diminished at three weeks following treatment as reported previously (40).

Pressure-volume Curves and Dynamic Respiratory Mechanics

Fig. 2 compares the quasi-static P-V curves in the two groups obtained during volume-controlled inflation from end-expiratory volume. The pressure was significantly lower in the PPE-treated mice than in the control ($P < 0.001$). The average quasi-static elastance value, defined as a slope between 0 and 1.15 ml of inflated volume, was significantly lower in the PPE-treated mice (18.8 ± 2.8 cmH_2O/ml) than in the control (26.5 ± 1.7 cmH_2O/ml) ($P < 0.001$).

Fig. 3 shows representative cases of the dynamic respiratory system resistance and elastance (calculated from the reactance where elastance = $-2\pi f$ * reactance) as a function of frequency, and the fits of the mathematical model (20) to the data in representative control and PPE-treated mice at PEEP = 3 cmH_2O. The measured data were fit well by the model at all PEEP levels in both groups. As a function of PEEP, all the values of tissue elastance (H) parameters, H_{min}, H_{max} and H_{mean}, were significantly PEEP-dependent ($P < 0.001$) and decreased with increasing PEEP in both groups (Fig. 4). The values of H_{min}, H_{max}, and H_{mean} were significantly lower in the PPE-treated group than in the control ($P < 0.001$)(Fig. 4A and B). The largest difference in H_{max} between the

control and the PPE-treated mice was at the highest (9 cmH_2O) PEEP. Hysteresivity η was significantly PEEP-dependent in the PPE-treated mice ($P < 0.001$) but not in the control, and was significantly higher in the PPE-treated mice at PEEP ≥ 6 cmH_2O (Fig. 5A). Airway resistance R_{aw} was significantly PEEP-dependent ($P < 0.001$), but there was no significant difference between the groups ($P = 0.78$)(Fig. 5B). The tissue damping (G) was significantly PEEP-dependent ($P < 0.001$) and significantly lower in the PPE-treated mice ($P < 0.001$) (Fig. 5C).

Dynamic Nonlinearity

The harmonic distortion K_d, a measure of dynamic nonlinearity of the respiratory system, was significantly PEEP-dependent ($P < 0.001$) and decreased implying more linear behavior when PEEP was increased in both groups (Fig. 6). The K_d was significantly larger in the PPE-treated group than in the control ($P < 0.001$). Figure 7 shows the linear relationships between H_{min} or H_{max} and K_d including data from all PEEP levels. There were significant correlations between H_{min} and K_d both in the PPE-treated ($K_d = 0.51H_{min} – 1.56$)($P < 0.001$, $r = 0.83$) and control groups ($K_d = 0.36H_{min} – 2.21$) ($P < 0.001$, $r = 0.90$) (Fig. 7A). The slopes of the two lines were significantly different ($P < 0.05$). There were also significant correlations between H_{max} and K_d both in the PPE-treated ($K_d = 0.13H_{max} – 2.44$) ($P < 0.001$, $r = 0.86$) and the control mice ($K_d = 0.14H_{max} – 0.82$)($P < 0.001$, $r = 0.86$) (Fig. 7B). The two lines were nearly parallel and there was no significant difference in slopes between the two lines ($P = 0.48$) but the intercept of the PPE-treated group was relatively higher which nearly reached a statistical level ($P = 0.07$). There were also significant correlations between H_{mean} and K_d both in the PPE-treated ($K_d = 0.29H_{mean} – 2.04$) ($P < 0.001$, $r = 0.93$) and the control groups ($K_d = 0.23H_{mean} – 3.00$) ($P < 0.001$, $r = 0.94$), and the slopes of the two lines were significantly different ($P < 0.05$)

(data not shown). Following the PPE treatment, each point moved to the left at an equivalent PEEP, implying stronger nonlinearity per unit tissue elastance in the PPE-treated group.

Lung Tissue Failure Tests

Fig. 8 shows representative traces of parenchymal tissue strip failure tests from a PPE-treated and a control mouse. The stress in each tissue strip increased with strain until a maximum was reached. Next, the stress started to drop in discrete steps suggesting that groups of alveolar walls broke within the tissue. Finally, the stress levels returned to zero when the samples separated into two pieces. Table 1 shows the summary of failure test results for all parenchymal tissue strips. The stress that developed just prior to the strips failing, defined as the failure stress, was significantly lower by 40% in the PPE-treated group than in the control ($P = 0.002$), demonstrating that the PPE-treated parenchymal tissues were weaker than control tissues. There were no significant differences in the strain values at failure ($P = 0.56$).

Lung Hydroxyproline and Elastin Levels

The levels of hydroxyproline and α-elastin are expressed as μg/mg dry weight of lung tissue (Table 2). There were no significant differences in dry lung weight between the control and the PPE-treated mice ($P = 0.81$). The levels of hydroxyproline, a measure of total collagen, were significantly higher in the PPE-treated mice by 48% than in the control ($P = 0.002$). The levels of α-elastin were lower by 13% in the PPE-treated mice, but the difference was not statistically significant ($P = 0.16$).

DISCUSSION

The primary findings of this study are that following PPE-treatment of mice (1) lung elastance decreased and hysteresivity increased, (2) parenchymal tissue fibers failed at a lower stress than in control, (3) dynamic nonlinearity characterized by harmonic distortion (K_d) increased, and (4) total collagen content increased while there was a tendency of loss of elastin of whole lungs in the emphysema group. These physiological observations support the hypothesis that exposure of the lung to PPE leads to a remodeling of the fiber network that significantly alters the mechanical properties and the nonlinear mechanical behavior of the whole organ.

Collagen Remodeling in Emphysema

In emphysema, the loss of elastin from the alveolar walls appears to be a major event in clinical pathology (1). The breakdown and the degradation of collagen fibers have also reported both in human patients (39) and in rodent models of emphysema (9, 35, 52). Additionally, several studies have demonstrated that after the destruction of alveolar walls, remodeling of collagen fibers as a result of an abnormal repair process contributes to the pathogenesis of emphysema (12, 17, 21, 22, 25, 49). Increases in total amount of collagen of the lungs have been reported in human patients (23, 35). In the present mouse model of emphysema, we also observed a 45% statistically significant increase in total collagen content and a 13% decrease in total elastin content of the whole lung (Table 2), suggesting that collagen remodeling within the lung was indirectly triggered following the elastolytic injury. Previous studies have shown that following the onset and initial progression of emphysema due to the proteolytic injury caused by PPE, synthesis of collagen by lung fibroblasts is considered to be upregulated as part of the repair process of the damaged lung (15, 22). However, the repair process does not restore normal structure and function to the lung leading to pathology and altered physiology (24). Since

the extracellular assembly of collagen molecules to fibrils and fibers is sensitive to the composition of the surrounding matrix (22, 24), it is conceivable that the structure and mechanical properties of the newly synthesized collagen differs from those that occur during normal growth. While the details of this abnormal repair process at the molecular level is beyond the scope of the present study, it is important to discuss the physiological consequences.

Alveolar Wall and Fiber Failure in Emphysema

It has long been proposed that mechanical failure of the alveolar walls plays a pivotal role in the progression of emphysema (50). Recently, Kononov et al. (21) observed the failure of a single alveolar wall in a rat model of PPE-induced emphysema. However, to our knowledge, this is the first study to quantify the failure stress of parenchymal tissue strips from emphysematous lungs. We found evidence that the emphysematous lung tissue breaks at the same strain, but at a stress 40% smaller than the normal tissue (Table 1). In an attempt to interpret these results, we first note that normal collagen fibers are stiffer and stronger than other connective tissue constituents (36). As a consequence, the amount and organization of collagen in the alveolar walls should play a crucial role in determining the stiffness and the failure properties of the lung tissue. For example, when the collagen content of normal lung tissue strips was decreased via *in vitro* digestion using collagenase, the stiffness of the tissue dropped to 40% of its value before digestion (53). Alternatively, normal developmental changes of the lung increase both the stiffness and the failure strength of the alveolar walls as well as collagen contents during maturation. Indeed, Tanaka and Ludwig (47) reported that the failure stress of normal lung tissue from baby rats was 18 kPa which increased to 28 kPa in adult rats. At the same time, in a follow-up study, Tanaka et al. (46) also found that the collagen content of the

lung increased from 18% to about 38% during this normal maturation process. Thus, since in this model of emphysema we found a 45% increase in lung collagen (Table 2), one would expect the stiffness and the failure stress of the tissue to increase. Surprisingly however, our data showed just the opposite behavior: despite the increase in collagen content, both lung elastance and the failure stress decreased by about 30% (Figs. 2 and 4) and 40% (Table 1), respectively, indicating that the total amount of collagen in the lung tissue is not the primary determinant of the mechanical properties in the diseased state.

In an attempt to resolve the apparent contradiction between increased collagen content and decreased elastance and failure stress in the emphysematous tissue, we first discuss the relation of lung stiffness and alveolar structure. Since the MLI nearly doubled in the emphysematous group, the number of alveolar walls per unit volume that can resist the deformation of the tissue strip could have decreased. This mechanism alone could account for the lower elastance and lower failure stress even if the mechanical properties of the alveolar walls were similar to those of the normal tissue. However, it is likely that not all of the increase in MLI is due to alveolar wall rupture. The PPE treated lung is softer and at the fixation pressure of 25 cmH_2O the alveoli would be more extended than those in the normal lung. Thus, the number of alveolar walls per unit volume in the tissue strip is not necessarily smaller in the PPE treated lung than in the normal. Using microscopic imaging, Brewer et al. (3) recently reported that individual alveolar walls from PPE-treated rats, which also involved collagen remodeling (21), appeared softer and more extensible than those from normal rats. These observations suggest that despite the increased collagen content, the alveolar walls and the collagen fibers are likely to be weaker in the emphysematous lung as a consequence of the process of degrading and remodeling. Indeed, the ultrastructure of collagen from human emphysematous lungs reveals thickened and disorganized fibrils after remodeling (12). Our data then suggest

that the stiffness and the failure properties of the remodeled fibers must decrease compared to normal collagen fibers.

The reduction in the failure stress of collagen has an important effect on how the structure of the lung evolves during the progression of emphysema. Suki et al. (44) recently developed a fiber network model and argued that since mechanical forces influence the process of tissue breakdown, the alveolar structure must be very heterogeneous and the alveolar walls around the perimeter of severe emphysema lesions or the walls that separate such lesions may be overstretched. In agreement with these predictions, the heterogeneity of the alveolar dimensions was found to be much larger in the emphysematous than in the control lungs, both in the current study and in previous studies (10, 20, 34). Therefore, the alveolar walls in the emphysematous lung may have to oppose larger stresses locally, and as a result, the increased local stresses can promote rupture of the remodeled walls (44), which in turn results in a decreased failure stress observed in Table 1. We thus conclude that mechanical forces are expected to play an important role in the progression of emphysema once the collagen matrix has undergone a critical amount of remodeling.

Lung Mechanical Properties

The consequences of alterations in the ECM of alveolar walls can be traced to organ level changes in the mechanical properties of the lung. Since the chest wall is very soft in the mouse, at least 90% of H is due to the lung parenchyma (37). Additionally, any change in H must be related to a change in lung mechanics and hence in the discussion that follows we assume that changes in H largely reflect changes in lung mechanics. We have recently developed a new mathematical model which assumes a continuous distribution of H between a minimum and a maximum value (H_{min} and H_{max}, respectively) (20). We found

that all H-related parameters (Fig. 4) as well as the static elastance (Fig. 2) decreased in the emphysematous mice compared to controls. The H_{max} represents the stiffest regional elastance in the lung and the collagen should be the most important determinant of its value. Thus, the lower H_{max} values in the PPE-treated mice suggest that the ultrastructural changes of remodeled collagen weakens the fibers and the alveolar walls in agreement with the analysis of the failure tests. On the other hand, we speculate that H_{min} represents the softest regional elastance, which may be related to the loss of alveolar walls in that region. Thus, it is likely that the lower value of H_{min} is a functional consequence of the increased MLI in the emphysematous mice.

The hysteresivity is a material property of the lung tissue (14) and it also depends on the microscopic constituents of the alveolar walls. Indeed, changes in ECM composition can cause a change in the hysteresivity in the parenchymal tissue level (33, 53). In the present study, hysteresivity of the PPE-treated mice was higher than that of the control mice, as observed in TGF-α transgenic emphysematous mice (32), in mild emphysematous mice induced by nebulized PPE-treatment (20) as well as in rats (3). In parenchymal tissues of normal guinea pigs, hysteresivity after *in vitro* digestion with collagenase was significantly higher than that after digestion with elastase (53). This suggests that in the normal lung tissue, the larger the elastin-to-collagen ratio the larger the value of hysteresivity. However, compared to controls, hysteresivity of the emphysematous mice increased (Fig. 5A) while collagen content also increased (Table 2). Taken together, the hysteresivity and elastance results suggest that remodeling in emphysema produces weak and viscous alveolar walls that also fail at lower stresses than those of the normal lung.

The values of R_{aw} decreased with increasing PEEP most likely due to the increasing diameters of the airways with lung inflation in both groups (Fig. 5B).

Although increased R_{aw} values, which suggest an underlying airway obstruction, were reported in sheep with experimental emphysema following papain treatment (19), R_{aw} values were the same between the groups, perhaps because the effects of PPE treatment on the airways used in this murine model is distinct from that of papain that was used in the ovine model. To our knowledge, increases in R_{aw} have not been reported in mouse models of emphysema yet. In another emphysema model of surfactant protein D deficient mice, R_{aw} became lower than in control (5). Thus, the physiological feature of the present model is similar to the classical physiological alterations in patients with α_1-antitrypsin deficiency (2), in which airway conductance was within normal limits, and the primary physiologic defect was a loss of elastic recoil.

Since surfactant plays an important role in the mechanical properties of the normal lung, it is conceivable that alterations in surfactant properties in the emphysematous lung could influence our results. Because fewer type II pneumocytes that secrete surfactant were observed in the lungs of human emphysema patients (31), it has been suggested that surfactant plays a protective role against the development of pulmonary emphysema. In PPE-treated mice, administration of surfactant prevents the development of emphysema (30). However, it is not known whether the composition and biophysical properties of lung surfactant change as a consequence of the development of emphysema. While the expression of surfactant protein A messenger RNA is increased in the lungs of the klotho mouse model of emphysema (41), this protein plays a less important role in stabilizing the alveoli than the hydrophobic surfactant proteins (18). One could argue that due to the reduction in lung tissue recoil, surface tension may become even more important in emphysema than in the normal lung. However, emphysema is associated with pronounced heterogeneity at the alveolar level, and it is unclear whether abnormalities in surfactant actually contribute to the development of the

disease. The extent to which lung surfactant contributes to recoil in emphysema has also not been well characterized. Further studies would be needed to clarify the role of surfactant in emphysema.

Dynamic Nonlinearities

Another important physiological finding of this study is that the tissues responsible for generating elastic recoil in the emphysematous lungs also displayed significantly greater nonlinear behavior than control lungs. The mechanical behavior of the normal lung tissue has been characterized as nonlinear (28, 29, 42, 53), and the origin of dynamic nonlinearity has been investigated in various organs (11). In the respiratory system, dynamic nonlinearity is likely related to the ECM components, including the nonlinearly viscoelastic collagen and its interactions with the linear viscoelastic elastin, and the viscous ground substance including mainly proteoglycans (29). Since elastic fibers behave more linearly than collagen fibers (28, 36), tissue nonlinearity could be more related to collagen and in particular, the extent to which collagen fibers are stretched in the alveolar walls. Thus, the dynamic nonlinear behavior of the lung tissue can be considered as a global *in vivo* assay of collagen function in the intact lung. While the nonlinearity is certainly related to collagen, it is also possible that the physical interaction between collagen and elastin also influences nonlinear behavior.

In the present study, we demonstrated for the first time that dynamic nonlinearity of the lung, as characterized by the harmonic distortion index K_d (42), is linearly related to lung elastance parameters (H_{min} and H_{max}) both in the PPE-treated and the control mice (Fig. 7), as found for normal tissue strips (53). More importantly, despite a decrease in H, the K_d increased in emphysema compared to normal lungs. Specifically, the relationship between K_d and H_{min} as well as H_{max} shifted to the left in emphysema. This can be

accounted for by changes in ECM components. As discussed above, a decrease in elastance and an increase in collagen content suggest that the new collagen in the remodeled alveolar walls must be less stiff than the normal collagen. An increase in K_d on the other hand, suggests that the collagen fibers are either more stretched or inherently different from normal with respect to their nonlinear mechanical behavior in the emphysematous alveolar wall.

One may argue that in contrast to tissue strips, in the whole lung airway closure also contributes to harmonic distortion. If a significant portion of the lung is blocked by airway closure and tidal volume remains the same, then a smaller lung will receive the same tidal volume and the lung becomes overstretched. In fact, the K_d was largest at PEEP = 0 in both groups (Fig. 6), which is the condition where recruitment and derecruitment could occur most during oscillations. Furthermore, the decrease in K_d with PEEP implies gradual recruitment. However, neither lung elastance nor K_d decreased when PEEP was increased from 6 to 9 cmH_2O. Thus, these data suggest that above 6 cmH_2O PEEP, recruitment did not occur and hence it could not influence our data. Therefore, we believe that the relation between K_d and H and consequently the above interpretation of the results, is insensitive to airway closure at least at the higher PEEPs included in this study.

In summary, we have characterized the respiratory and lung mechanical properties of a mouse model of emphysema induced by PPE. We observed a decrease in lung elastance and failure strength of the alveolar walls as well as an increase in hysteresivity, dynamic nonlinearity and total lung collagen content. These results suggest that significant collagen remodeling takes place within the alveolar wall, which produces weak but more nonlinear fibers and alveoli that are locally overstretched and hence prone

to mechanical failure. These alterations in the micromechanics of the alveolar walls significantly affect organ level lung function in the mouse.

ACKNOWLEDGEMENT

This study was funded by National Heart, Lung, and Blood Institute Grant HL 59215-04.

REFERENCES

1. Barnes PJ. Chronic obstructive pulmonary disease. *N Engl J Med* 343: 269-280, 2000.
2. Black LF, Hyatt RE, and Stubbs SE. Mechanism of expiratory airflow limitation in chronic obstructive pulmonary disease associated with α1-antitrypsin deficiency. *Am Rev Respir Dis* 105: 891-899, 1972.
3. Brewer KK, Sakai H, Alencar AM, Majumdar, Arold SP, Lutchen KR, Ingenito EP, and Suki B. Lung and alveolar wall elastic and hysteretic behavior in rats: effects of in vivo elastase treatment. *J Appl Physiol* 95: 1926-1936, 2003.
4. Cardoso WV, Sekhon HS, Hyde DM, and Thurlbeck WM. Collagen and elastin in human pulmonary emphysema. *Am Rev Respir Dis* 147: 975-981, 1993.
5. Collins RA, Ikegami M, Korfhagen TR, Whitsett JA, and Sly PD. In vivo measurements of changes in respiratory mechanics with age in mice deficient in surfactant protein D. *Pediatr Res* 53: 463-467, 2003.
6. Csendes T. Nonlinear parameter estimation by global optimization: efficiency and reliability. *Acta Cybernetica* 8: 361-370, 1988.
7. Cunningham L, and Frederiksen D. Elastin structure and biosynthesis. *Methods Enzymol* 82: 559-743, 1982.
8. D'Armiento J, Dalal SS, Okada Y, Berg RA, and Chada K. Collagenase expression in the lungs of transgenic mice causes pulmonary emphysema. *Cell* 71:955-961, 1992.
9. Dhami R, Gilks B, Xie C, Zay K, Wright J, and Churg A. Acute cigarette smoke-induced connective tissue breakdown is mediated by neutrophils and prevented by α1-antitrypsin. *Am J Respir Cell Mol Biol* 22: 244-252, 2000.

10. Dunnill MS. Quantitative methods in the study of pulmonary pathology. *Thorax* 17: 320-328, 1962.

11. Fee MS, Shraiman B, Pesaran B, and Mitra PP. The role of nonlinear dynamics of the syrinx in the vocalizations of a songbird. *Nature* 395: 67-71, 1998.

12. Finlay GA, O'Donnell MD, O'Connor CM, Hayes JP, and FitzGerald MX. Elastin and collagen remodeling in emphysema: A scanning electron microscopy study. *Am J Pathol* 149: 1405-1415, 1996.

13. Foronjy RF, Okada Y, Cole R, and D'Armiento J. Progressive adult-onset emphysema in transgenic mice expressing human MMP-1 in the lung. *Am J Physiol Lung Cell Mol Physiol* 284: L727-L737, 2003.

14. Fredberg JJ, and Stamenovic D. On the imperfect elasticity of lung tissue. *J Appl Physiol* 67: 2408-2419, 1989.

15. Gardi C, Calzoni P, Marcolongo P, Cavarra E, Vanni L, and Lungarella G. Collagen breakdown products and lung collagen metabolism: an in vitro study on fibroblast cultures. *Thorax* 49: 312-318, 1994.

16. Hantos Z, Daroczy B, Suki B, Nagy S, and Fredberg JJ. Input impedance and peripheral inhomogeneity of dog lungs. *J Appl Physiol* 72: 168-178, 1992.

17. Hogg JC, and Senior RM. Chronic obstructive pulmonary disease - part 2: pathology and biochemistry of emphysema. *Thorax* 57: 830-834, 2002.

18. Ingenito EP, Mark L, Morris J, Espinosa FF, Kamm RD, and Johnson M. Biophysical characterization and modeling of lung surfactant components. *J Appl Physiol* 86:1702-14, 1999.

19. Ingenito EP, Reilly JJ, Mentzer SJ, Swanson SJ, Vin R, Keuhn H, Berger RL, and Hoffman A. Bronchoscopic volume reduction: a safe and effective alternative to surgical therapy for emphysema. *Am J Respir Crit Care Med* 164: 295-301, 2001.

20. Ito S, Ingenito EP, Arold SP, Parameswaran H, Tgavalekos NT, Lutchen KR, and Suki B. Tissue heterogeneity in the mouse lung: effects of elastase treatment. *J Appl Physiol* 97:204-212, 2004.

21. Kononov S, Brewer K, Sakai H, Cavalcante FSA, Sabayanagam C, Ingenito EP, and Suki B. Roles of mechanical forces and collagen failure in the development of elastase-induced emphysema. *Am J Respir Crit Care Med* 164: 1920-1926, 2001.

22. Kuhn C, Yu SY, Chraplyvy M, Linder HE, and Senior RM. The induction of emphysema with elastase: changes in connective tissue. *Lab Invest* 34: 372-380, 1976.

23. Lang MR, Fiaux GW, Gillooly M, Stewart JA, Hulmes DJ, and Lamb D. Collagen content of alveolar wall tissue in emphysematous and non-emphysematous lungs. *Thorax* 49: 319-326, 1994.

24. Laurent GJ. Regulation of lung collagen production during wound healing. *Chest* 99: 67S-69S, 1991.

25. Lucey EC, Goldstein RH, Stone PJ, and Snider GL. Remodeling of alveolar walls after elastase treatment of hamsters: Results of elastin and collagen mRNA *in situ* hybridization. *Am J Respir Crit Care Med* 158: 555-564, 1998.

26. Lucey EC, Kean J, Kuang P, Snider GL, and Goldstein RH. Severity of elastase-induced emphysema is decreased in tumor necrosis factor-α and interleukin-1β receptor deficient mice. *Lab Invest* 82: 79-85, 2002.

27. Lutchen KR, Yang K, Kaczka DW, and Suki B. Optimal ventilator waveform for estimating low-frequency respirator impedance in healthy and diseased subjects. *J Appl Physiol* 75: 478-488, 1993.

28. Maksym GN, and Bates JHT. A distributed nonlinear model of lung tissue elasticity. *J Appl Physiol* 82: 32-41, 1997.

29. Navajas D, Maksym GN, and Bates JHT. Dynamic viscoelastic nonlinearity of lung parenchymal tissue. *J Appl Physiol* 79: 348-356, 1995.

30. Otto-Verberne CJ, Ten Have-Opbroek AA, Franken C, Hermans J, and Dijkman JH.Protective effect of pulmonary surfactant on elastase-induced emphysema in mice. *Eur Respir J* 5: 1223-1230, 1992.

31. Otto-Verberne CJ, Ten Have-Opbroek AA, Willems LN, Franken C, Kramps JA, and Dijkman JH. Lack of type II cells and emphysema in human lungs. *Eur Respir J* 4: 316-323, 1991.

32. Pillow JJ, Korfhagen TR, Ikegami M, and Sly PD. Overexpression of TGF-α increases lung tissue hysteresivity in transgenic mice. *J Appl Physiol* 91: 2730-2734, 2001.

33. Rocco PRM, Negri EM, Kurtz PM, Vasconcellos FP, Silva GH, Capelozzi VL, Romero PV, and Zin WA. Lung tissue mechanics and extracellular matrix remodeling in acute lung injury. *Am J Respir Crit Care Med* 164: 1067-1071, 2001.

34. Russi EW, Bloch KE, and Weder W. Functional and morphological heterogeneity of emphysema and its implication for selection of patients for lung volume reduction surgery. *Eur Respir J* 14: 230-236, 1999.

35. Selman M, Montano M, Ramos C, Vanda B, Becerril C, Delgado J, Sansores R, Barrios R, and Pardo A. Tobacco smoke-induced lung emphysema in guinea pigs is associated with increased interstitial collagenase. *Am J Physiol Lung Cell Mol Physiol* 271: L734-L743, 1996.

36. Silver, F, Horvath I, and Foran D. Viscoelasticity of the vessel wall: the role of collagen and elastic fibers. *Crit Rev Biomed Eng* 29: 279-301, 2001.

37. Sly PD, Collins RA, Thamrin C, Turner DJ, and Hantos Z. Volume dependence of airway and tissue impedances in mice. *J Appl Physiol* 94: 1460-1466, 2003.

38. Snider GL, Lucy EC, and Stone PJ. Animal models of emphysema. *Am Rev Respir Dis* 133: 149-169, 1986.

39. Stone PJ, Gottlier DJ, O'Connor GT, Ciccolella DE, Breuer R, Bryan-Rhadfi J, Shaw HA, Franzblau C, and Snider GL. Elastin and collagen degradation products in urine of smokers with and without chronic obstructive pulmonary disease. *Am J Respir Crit Care Med* 151: 952-959, 1995.

40. Stone PJ, Lucey EC, Calore JD, McMahon MP, Snider GL, and Franzblau C. Defenses of the hamster lung against human neutrophil and porcine pancreatic elastase. *Respiration* 54: 1-15, 1988.

41. Suga T, Kurabayashi M, Sando Y, Ohyama Y, Maeno T, Maeno Y, Aizawa H, Matsumura Y, Kuwaki T, Kuro-O M, Nabeshima Y, and Nagai R. Disruption of the klotho gene causes pulmonary emphysema in mice. Defect in maintenance of pulmonary integrity during postnatal life. *Am J Respir Cell Mol Biol* 22: 26-33, 2000.

42. Suki B, Hantos Z, Daroczy B, Alkaysi G, and Nagy S. Nonlinearity and harmonic distortion of dog lungs measured by low-frequency forced oscillations. *J Appl Physiol* 71: 69-75, 1991.

43. Suki B, and Lutchen KR. Pseudorandom signals to estimate apparent transfer and coherence functions of nonlinear systems: applications to respiratory mechanics. *IEEE Trans Biomed Eng* 39: 1142-1151, 1992.

44. Suki B, Lutchen KR, and Ingenito EP. On the progressive nature of emphysema: roles of proteases, inflammation, and mechanical forces. *Am J Respir Crit Care Med* 168: 516-521, 2003.

45. Takubo Y, Guerassimov A, Ghezzo H, Triantafillopoulos A, Bates JH, Hoidal JR, and Cosio MG. α_1-Antitrypsin determines the pattern of emphysema and function in tobacco smoke-exposed mice: parallels with human disease. *Am J Respir Crit Care Med* 166: 1596-1603, 2002.

46. Tanaka R, Al-Jamal R, and Ludwig MS. Maturational changes in extracellular matrix and lung tissue mechanics. *J Appl Physiol* 91: 2314-2321, 2001.

47. Tanaka R, and Ludwig MS. Changes in viscoelastic properties of rat lung parenchymal strips with maturation. *J Appl Physiol* 87: 2081-2089, 1999.

48. van Straaten JFM, Coers W, Noordhoek JA, Huitema S, Flipsen JTM, Kauffman HF, Timens W, and Postma DS. Proteoglycan changes in the extracellular matrix of lung tissue from patients with pulmonary emphysema. *Mod Pathol* 12: 697-705, 1999.

49. Vlahovic G, Russel ML, Mercer RR, and Crapo JD. Cellular and connective tissue changes in alveolar septal walls in emphysema. *Am J Respir Crit Care Med* 160: 2086-2092, 1999.

50. West JB. Distribution of mechanical stress in the lung: possible factor in localization of pulmonary disease. *Lancet* 1: 839-841, 1971.

51. Woessner JF. The determination of hydroxyproline in tissue and protein samples containing small proportions of this imino acid. *Arch Biochem Biophys* 93: 440-447, 1961.

52. Wright JL, and Churg A. Smoke-induced emphysema in guinea pigs is associated with morphometric evidence of collagen breakdown and repair. *Am J Physiol Lung Cell Mol Physiol* 268: L17-L20, 1995.

53. Yuan H, Kononov S, Cavalcante FSA, Lutchen KR, Ingenito EP, and Suki B. Effects of collagense and elastase on the mechanical properties of lung tissue strips. *J Appl Physiol* 89: 3-14, 2000.

54. Zhang Q, Suki B, and Lutchen KR. Harmonic distortion from nonlinear systems with broadband inputs: applications to lung mechanics. *Ann Biomed Eng* 23: 672-681, 1995.

FIGURE LEGENDS

Fig. 1.

Examples of the alveolar structures of lung tissues from the control (A) and the porcine pancreatic elastase (PPE)-treated (B) lungs. Photographs were taken at an original magnification of x 50 from slides stained with hematoxylin and eosin.

Fig. 2.

Mean ± SD of quasi-static inspiratory pressure-volume relationships from end-expiratory lung volume of the control and the PPE-treated mice. Values are means ± SD. * $P < 0.05$.

Fig. 3.

Representative examples of respiratory system resistance (A) and elastance (B) of the control and the PPE-treated mice calculated from the impedance data and corresponding fits of the model to the control and PPE-treated data at a positive end-expiratory pressure (PEEP) of 3 cmH_2O.

Fig. 4.

Dynamic tissue elastance (H) parameters as a function of PEEP. Means ± SD of minimum (H_{min}), maximum (H_{max}) (A), and mean H (H_{mean}; B) in the control and PPE-treated mice. * $P < 0.05$.

Fig. 5.

Means ± SD of hysteresivity (A), airway resistance (R_{aw})(B), and tissue damping (G)(C) in the control and PPE-treated mice as a function of PEEP. * $P < 0.05$.

Fig. 6.

Harmonic distortion, an index of dynamic nonlinearity of the respiratory system, of the control and the PPE-treated mice as a function of PEEP. * $P < 0.05$.

Fig. 7.

Correlations between H_{min} (A) or H_{max} (B) and harmonic distortion. Data were obtained from of the control (n = 8) and the PPE-treated (n = 9) mice at PEEP = 0, 3, 6, and 9 cmH_2O.

Fig. 8.

Representative examples of parenchymal tissue failure tests of the control and the PPE-treated mice. Notice that the strain axis starts at 2.0. Arrows indicate failure points.

Table 1. *Tissue fiber rupture test*

	Failure stress (kPa)	Strain
Control	11.9 ± 1.4	3.33 ± 0.49
PPE-treated	7.2 ± 2.4	3.59 ± 0.93
	P = 0.002	P = 0.56

Data are expressed as means ± SD (n = 6 in each group). PPE; porcine pancreatic elastase.

Table 2. *Lung collagen and elastin contents*

	Dried lung weight (mg)	Hydroxyproline (μg/mg)	α-Elastin (μg/mg)
Control	13.5 ± 3.8	4.38 ± 0.83	47.2 ± 6.0
PPE-treated	13.1 ± 2.4	6.38 ± 1.33	41.2 ± 8.8
	P = 0.81	P = 0.002	P = 0.16

Data are expressed as means ± SD. Hydroxyproline and α-elastin contents are expressed as μg/mg of dried lung weight (n = 7 in each group).

Fig. 1A and B

A

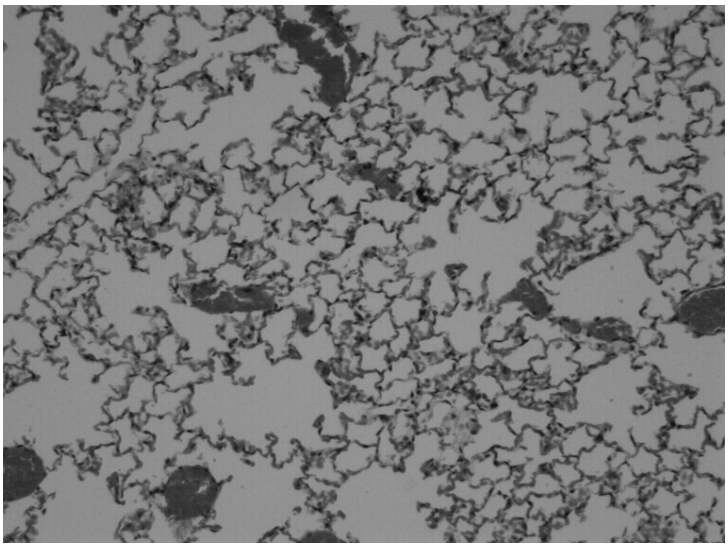

B

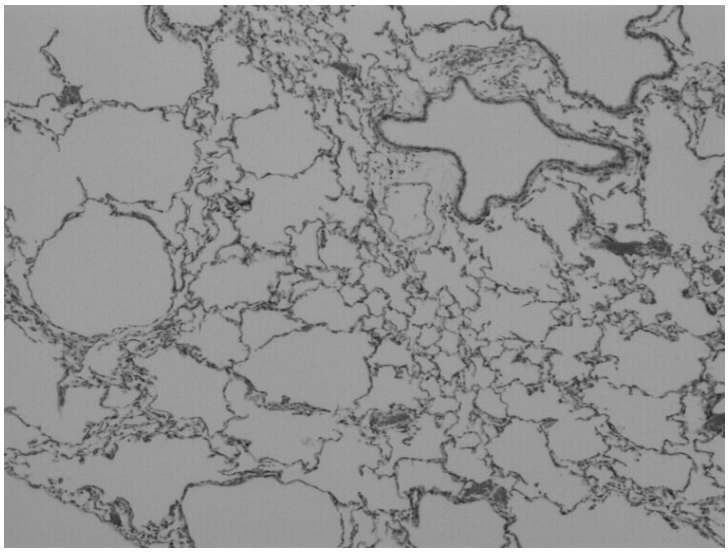

Fig. 2

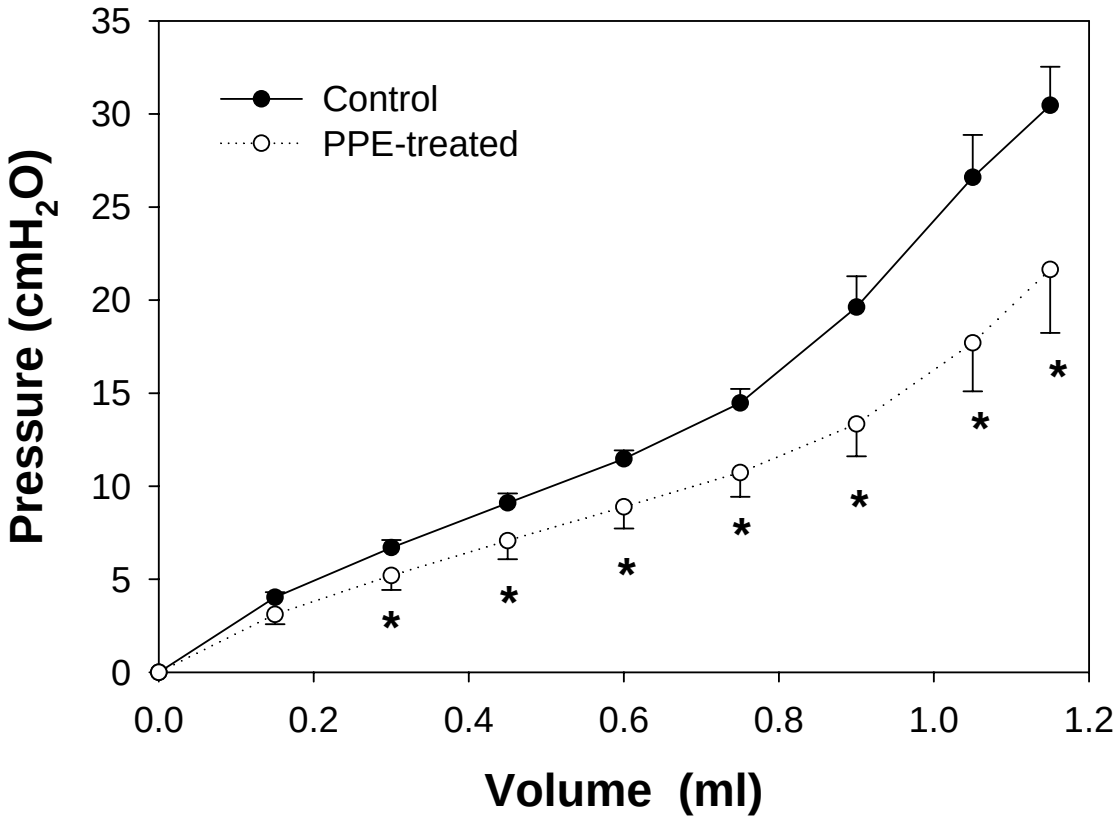
Control
PPE-treated
Pressure (cmH2O)
Volume (ml)
0
5
10
15
20
25
30
35
0.0
0.2
0.4
0.6
0.8
1.0
1.2
*

Fig. 3A and B

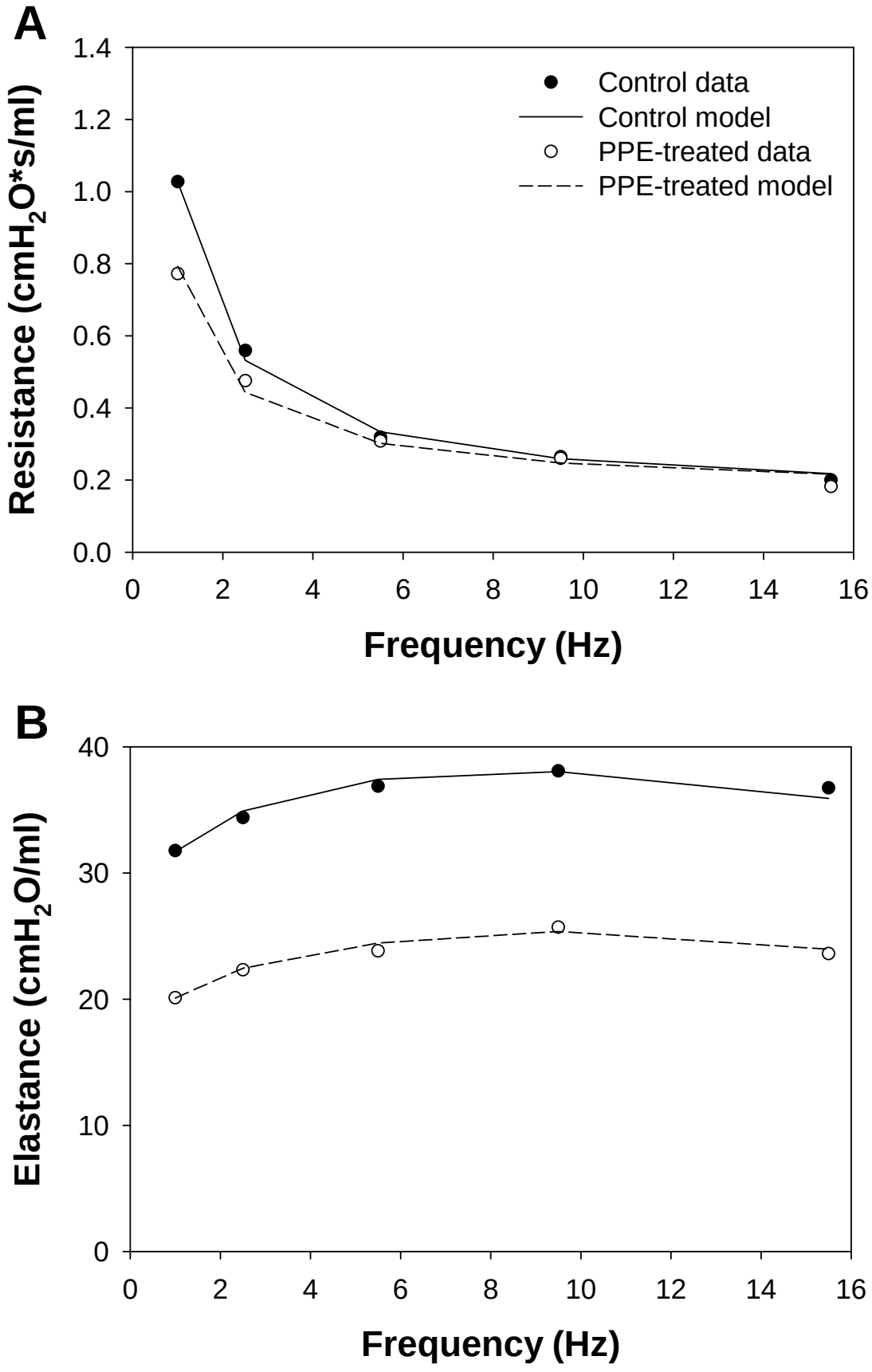
A
Resistance (cmH2O*s/ml)
1.4
1.2
1.0
0.8
0.6
0.4
0.2
0.0
0
2
4
6
8
10
12
14
16
Frequency (Hz)
Control data
Control model
PPE-treated data
PPE-treated model
B
Elastance (cmH2O/ml)
40
30
20
10
0
0
2
4
6
8
10
12
14
16
Frequency (Hz)

Fig. 4A and B

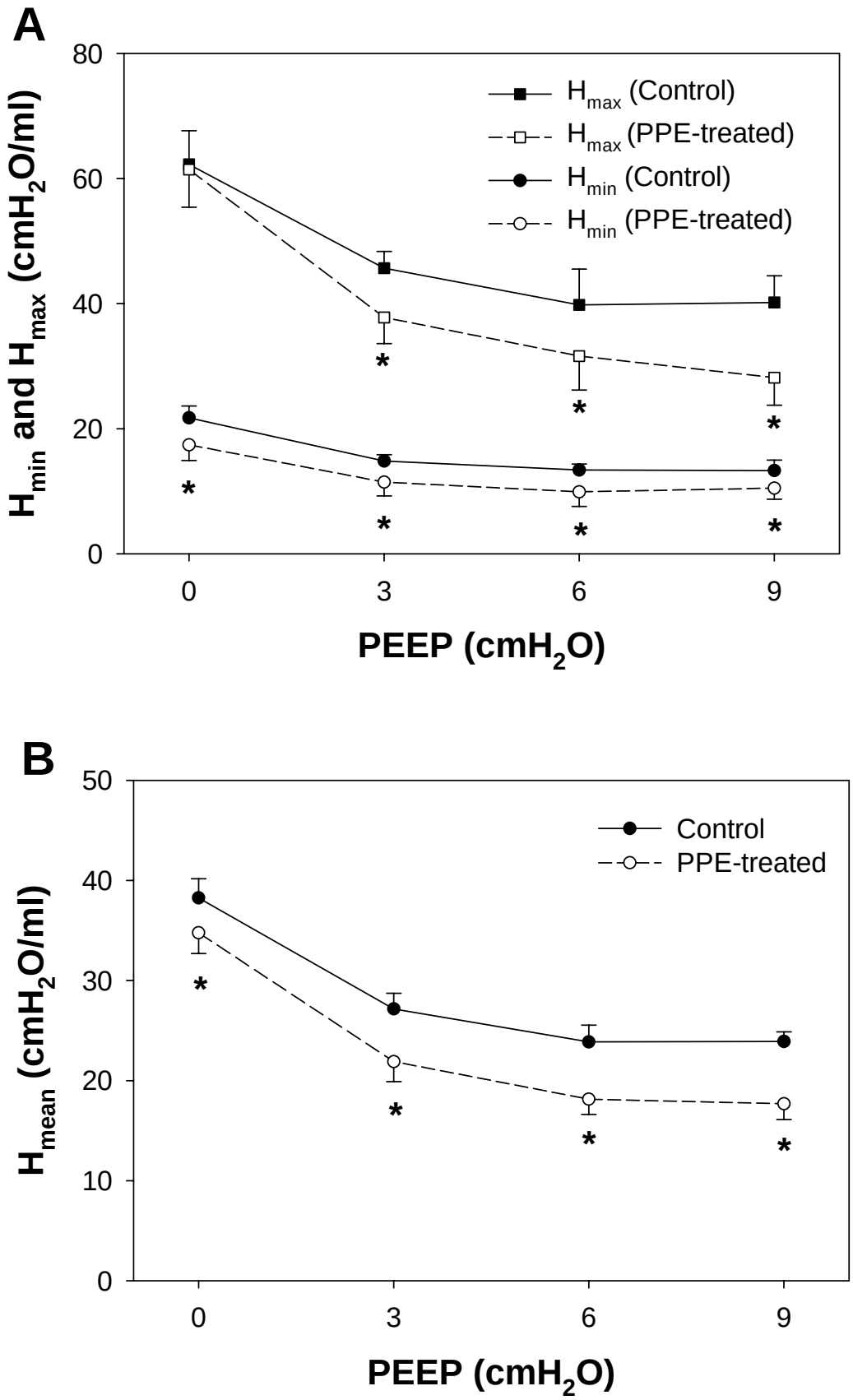
A
80
60
40
20
0
H_{min} and H_{max} (cmH_2O/ml)
H_{max} (Control)
H_{max} (PPE-treated)
H_{min} (Control)
H_{min} (PPE-treated)
*
0
3
6
9
PEEP (cmH_2O)
B
50
40
30
20
10
0
H_{mean} (cmH_2O/ml)
Control
PPE-treated
*
0
3
6
9
PEEP (cmH_2O)

Fig. 5A and B

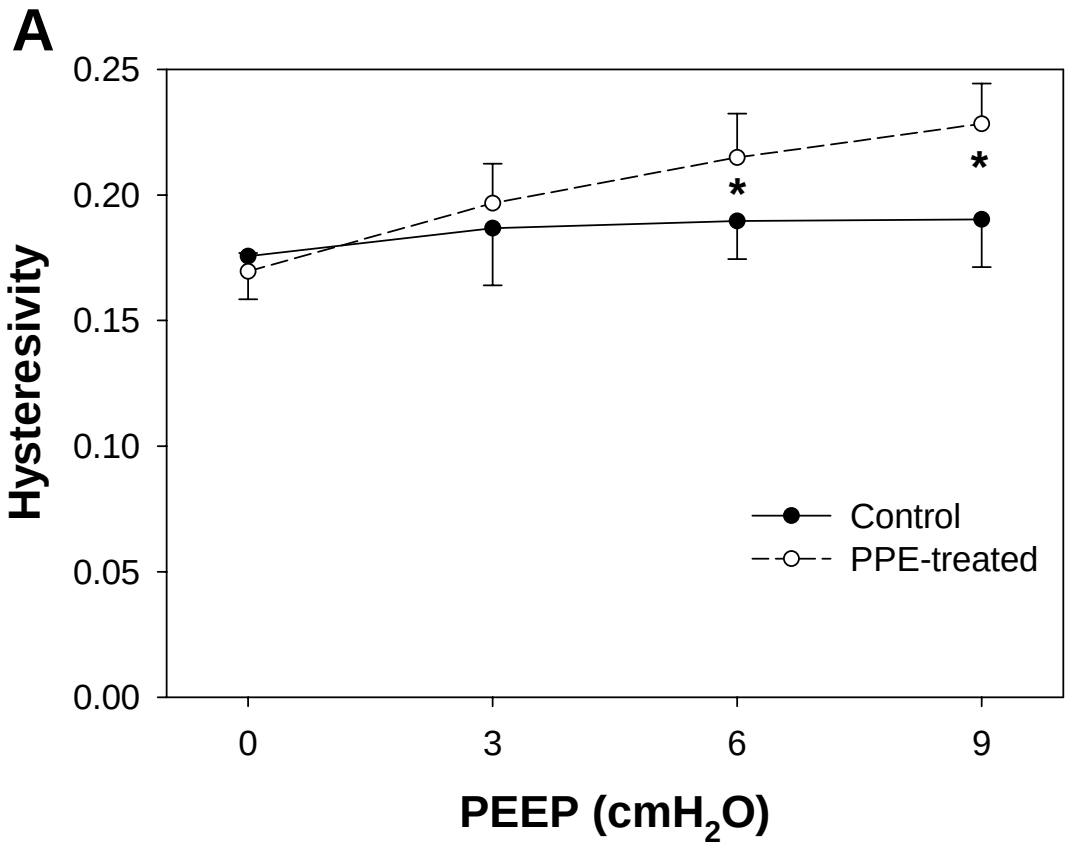
A
Hysteresivity
0.25
0.20
0.15
0.10
0.05
0.00
0
3
6
9
PEEP (cmH2O)
Control
PPE-treated
*
*

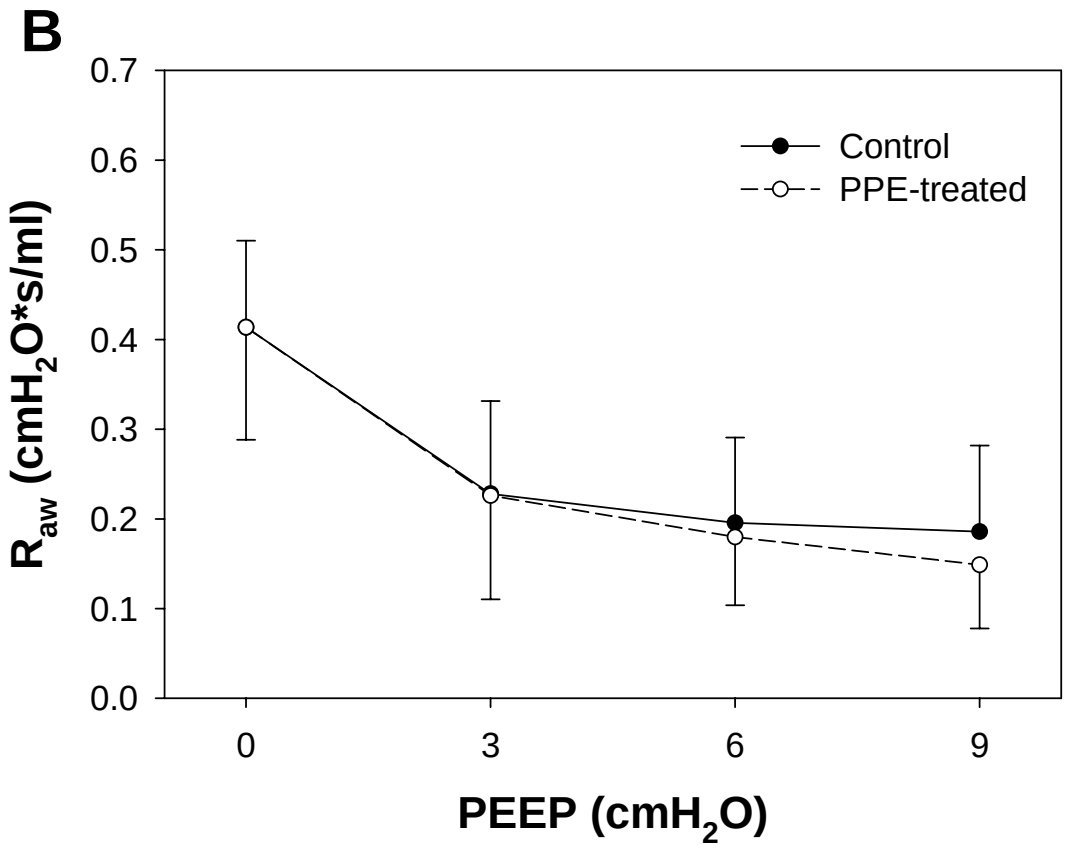
B
Raw (cmH2O*s/ml)
0.7
0.6
0.5
0.4
0.3
0.2
0.1
0.0
0
3
6
9
PEEP (cmH2O)
Control
PPE-treated

Fig. 5C

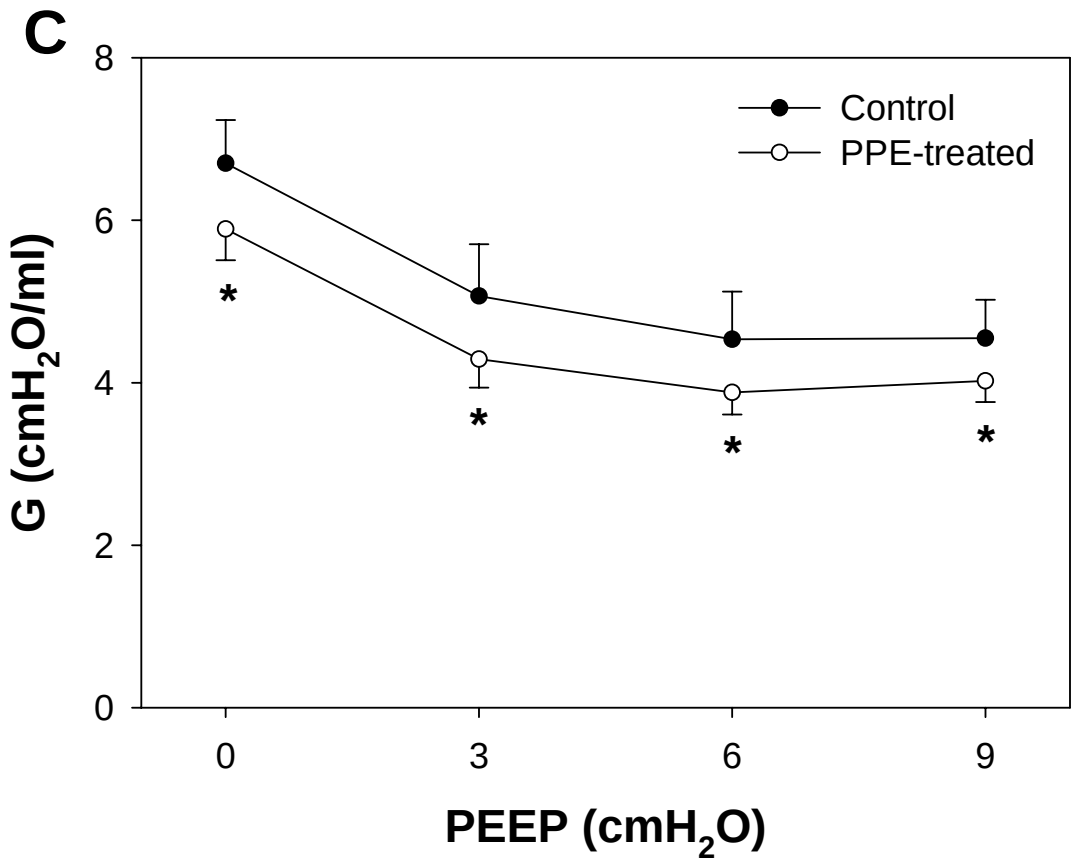

Fig. 6

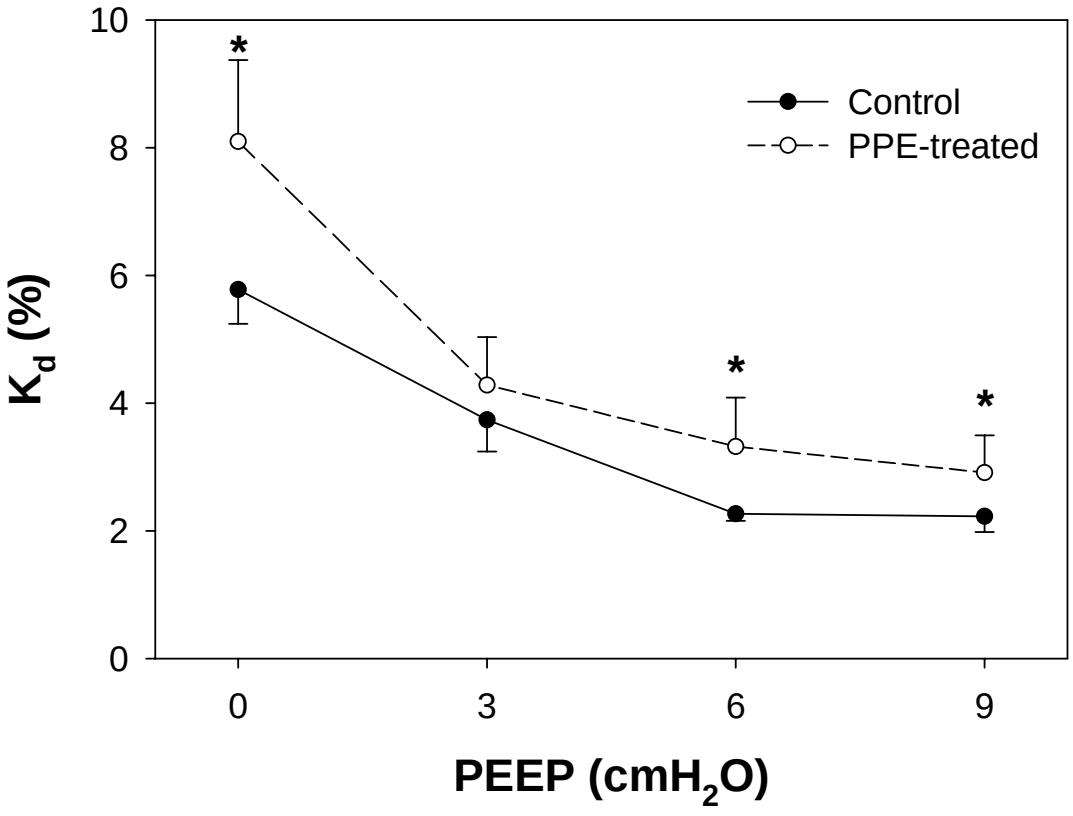

Fig. 7A and B

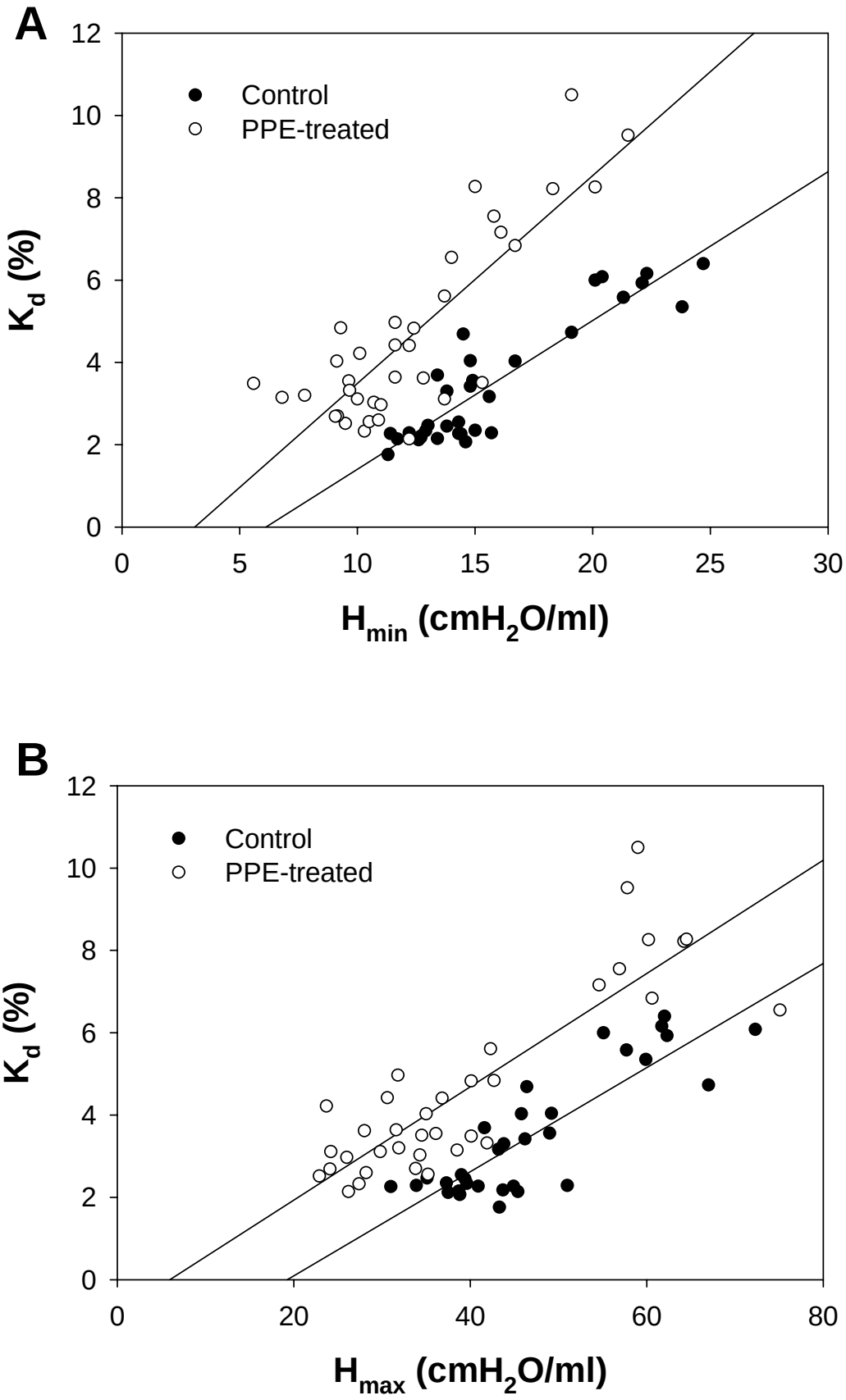
A
Control
PPE-treated
K_d (%)
H_{min} (cmH_2O/ml)
0
2
4
6
8
10
12
0
5
10
15
20
25
30
B
Control
PPE-treated
K_d (%)
H_{max} (cmH_2O/ml)
0
2
4
6
8
10
12
0
20
40
60
80

Fig. 8

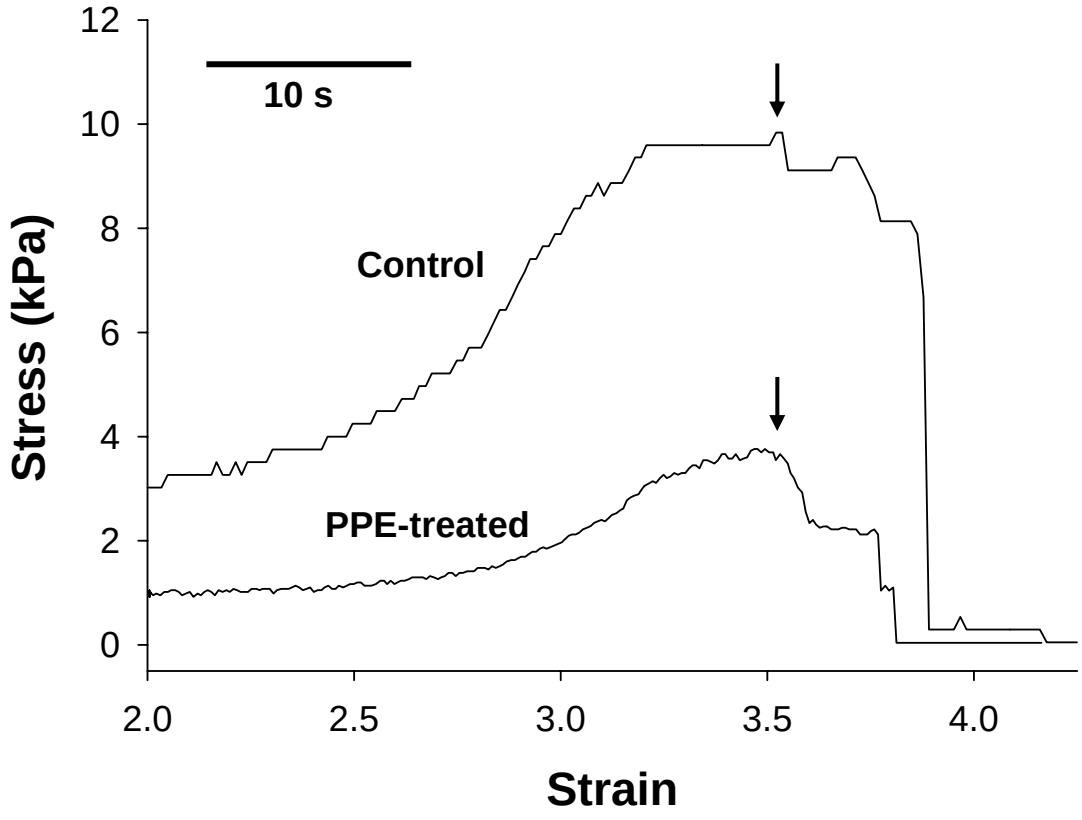
12
10
8
6
4
2
0
Stress (kPa)
10 s
Control
PPE-treated
2.0
2.5
3.0
3.5
4.0
Strain